

# Mechanistic Understanding of Polarization-Type Potential-Induced Degradation in Crystalline-Silicon Photovoltaic Cell Modules

Seira Yamaguchi,\* Atsushi Masuda, Kazuhiro Marumoto, and Keisuke Ohdaira

Potential-induced degradation (PID) has been identified as a central reliability issue of photovoltaic (PV) cell modules. Several types of PID depend on the cell structure. Among those types, polarization-type PID, which is characterized by reductions in short-circuit current density ( $J_{sc}$ ) and open-circuit voltage ( $V_{oc}$ ), is the fastest PID mode. Additionally, polarization-type PID occurs readily at room temperature or at markedly low magnitudes of electric potential difference. Therefore, polarization-type PID is a severe difficulty affecting silicon PV modules. Recently, degradation behavior, preventive measures, and mechanism have been investigated. As described herein, mechanistic aspects of polarization-type PID are specifically examined and details of a recently proposed model involving a charge accumulation process at K centers in  $SiN_x$  dielectric layers: the K-center model are discussed. The K-center model consistently explains previously reported results of experimentation, which indicates the validity of this model. Discussions presented herein are expected to improve the mechanistic understanding of polarization-type PID in the PV community and to stimulate further discussions and verifications of the model.

for crystalline-silicon (c-Si) PV technologies, these improvements are crucially important because the highest power-conversion efficiency (PCE) has reached 26.7%,<sup>[1]</sup> which is approaching the theoretical limit of 29%,<sup>[2]</sup> leaving less room for PCE improvement. In the field, PV cell modules can be subjected to various stresses and can experience various degradation processes, including potential-induced degradation (PID).<sup>[3–10]</sup> Consequently, long-term stability and reliability improvements demand a better understanding of the degradation mechanisms associated with these degradation processes.

As a practical matter, PID occurs mainly in large-scale photovoltaic systems. Conventional PV modules are generally composed of soda-lime glass as cover glass, ethylene–vinyl acetate (EVA) copolymer as an encapsulant, solar cells, a backsheet, and


an aluminum (Al) frame. Typically, many PV modules are connected in series in large-scale PV systems to build up the voltage output, whereas the module frames are grounded for safety reasons. The voltage is typically set to 1000 V or higher. The active circuits of cells in modules therefore have large positive or negative potentials with respect to the individual modules' grounded frame. These high electric potential differences might lead to

## 1. Introduction

Solar photovoltaic (PV) energy has been demonstrated as an important renewable energy resource for future sustainable social systems. The realization of such social systems requires improvement of PV cell and module technologies. These include improvements in long-term stability and reliability. Particularly

S. Yamaguchi, K. Marumoto  
Division of Materials Science  
Faculty of Pure and Applied Sciences  
University of Tsukuba  
Tsukuba, Ibaraki 305-8573, Japan  
E-mail: yamaguchi@ims.tsukuba.ac.jp

A. Masuda  
Graduate School of Science and Technology  
Niigata University  
Niigata 950-2181, Japan

 The ORCID identification number(s) for the author(s) of this article can be found under <https://doi.org/10.1002/aesr.202200167>.

© 2022 The Authors. Advanced Energy and Sustainability Research published by Wiley-VCH GmbH. This is an open access article under the terms of the Creative Commons Attribution License, which permits use, distribution and reproduction in any medium, provided the original work is properly cited.

DOI: 10.1002/aesr.202200167

A. Masuda  
Interdisciplinary Research Center for Carbon-Neutral Technology  
Niigata University  
Niigata 950-2181, Japan

K. Marumoto  
Tsukuba Research Center for Energy Materials Science  
University of Tsukuba  
Tsukuba, Ibaraki 305-8571, Japan

K. Ohdaira  
Graduate School of Advanced Science and Technology  
Japan Advanced Institute of Science and Technology  
Nomi, Ishikawa 923-1292, Japan

degradation, known as PID. One particularly important feature of PID is that considerable degradation occurs rapidly in the field, during as little as several months.<sup>[11]</sup> Degradation of this kind is therefore regarded as a central reliability issue in large-scale PV systems. Another important feature of PID is that the PID behavior varies considerably depending on PV cell materials, structures, and PID-stress intensity.<sup>[9,10]</sup> For instance, sodium-penetration-type PID (including shunting-type PID),<sup>[3–8,12]</sup> corrosion-type PID,<sup>[13–18]</sup> and polarization-type PID<sup>[12,19–34]</sup> are known to occur depending on these factors.

Among these, polarization-type PID, which is the first discovered PID type, is known to be the fastest PID mode. It has been observed in c-Si cells of several types, including n-type passivated emitter and rear totally diffused (PERT) cells,<sup>[20,23,24,26–28,31,32,34,35]</sup> n-type interdigitated back-contact (IBC) cells with a front surface field<sup>[19,25]</sup> or with a front floating emitter,<sup>[21]</sup> p-type passivated emitter and rear cells (PERCs),<sup>[28,29,33]</sup> and p-type conventional c-Si cells with Al back surface fields (Al-BSFs).<sup>[30,35]</sup> Figure 1 presents the representative structures of the n-type PERT cells, the n-type IBC cells, the p-type PERCs, and the p-type Al-BSF cells. It is noteworthy that these cells all have dielectric passivation layers with SiN<sub>x</sub>. Polarization-type PID is characterized by reductions in the short-circuit current density,  $J_{SC}$ , and in the open-circuit voltage,  $V_{OC}$ , as described in detail in Section 2. In accelerated PID tests conducted at 85 °C with a bias of –1000 V, polarization-type PID was observed to occur from the first few seconds.<sup>[23,26]</sup> Polarization-type PID also has a feature by which the temperature and voltage conditions necessary for its degradation are less stringent. For example, polarization-type PID has been reported to

occur even under room temperature conditions or under very low voltage conditions such as –50 V.<sup>[20]</sup> This feature suggests that this type of PID can occur even in small-scale systems such as rooftop PV systems or in systems with module-level power electronics, which is an undesirable feature that is not present in Na-penetration-type PID or corrosion-type PID. Furthermore, earlier reports have described some preventive measures as not very effective for polarization-type PID, such as the use of alternative module encapsulants.<sup>[20,27]</sup> These characteristics make polarization-type PID a more severe difficulty. Therefore, a better mechanistic understanding of polarization-type PID is crucially important for developing stable and reliable c-Si PV cell modules.

This article presents a review, with detailed discussion of the proposed mechanisms of polarization-type PID, based on reports from the literature. Section 2 gives a brief review of polarization-type PID behavior and important related results. Section 3 presents a detailed discussion of a proposed mechanism, the K-center model, including our conception of the model. Section 4 includes some examples for which the model explains experimentally obtained data. Section 5 presents a summary of the results obtained from this study.

## 2. Characteristic Behavior of Polarization-Type PID

Understanding characteristic degradation behavior is important because, in many cases, degradation behavior is the point of embarkation for understanding degradation mechanisms.

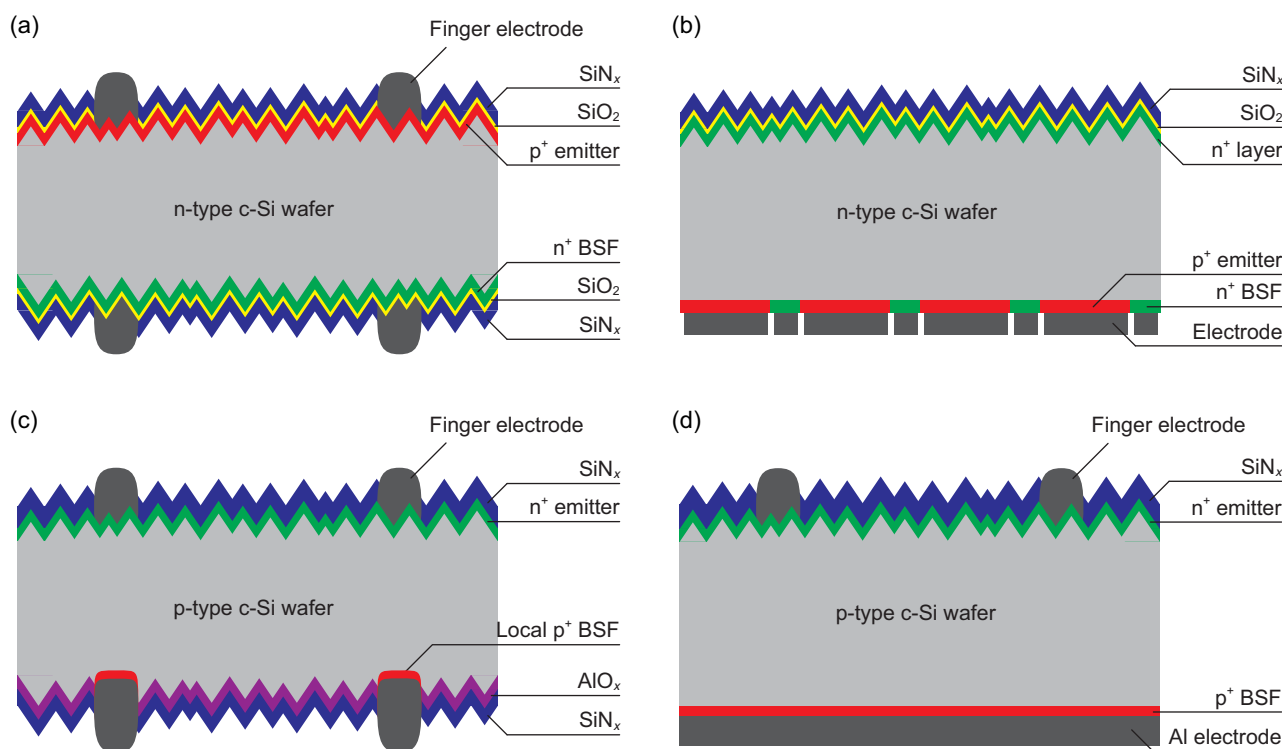


**Figure 1.** Schematic diagrams of cross sections of representative a) n-type front-emitter PERT, b) n-type IBC cells, c) p-type bifacial PERCs, and d) p-type Al-BSF cells (not to scale). Panels (a) and (b): Reproduced with permission.<sup>[10]</sup> Copyright 2021, Wiley-VCH GmbH.

Therefore, we explain the characteristic behaviors of polarization-type PID below.

Polarization-type PID is characterized by reductions in  $J_{SC}$  and  $V_{OC}$ .<sup>[20]</sup> Reduced  $J_{SC}$  limits the overall current of a series-connected circuit. Therefore, polarization-type PID causing  $J_{SC}$  reduction presents a severe difficulty. When polarization-type PID occurs on the front side of cells, the reductions are accompanied by reduction in the external quantum efficiency (EQE) in a short-wavelength range.<sup>[20]</sup> (Note that in this case, the light for the EQE measurement was illuminated on the front side of the cells.) However, polarization-type PID that occurs on the rear side of cells reduces EQE in a long-wavelength range with slight  $J_{SC}$  reduction.<sup>[29]</sup> Unlike the case of shunting-type PID, the fill factor (FF) remains unchanged for polarization-type PID in most cases. This fact implies that polarization-type PID does not affect the p–n junction interface of solar cells. It results from enhanced surface recombination.

One important feature is that polarization-type PID can occur under either bias. More precisely, the bias direction causing polarization-type PID changes depending on the doping type of the cell surface. For example, in the first report on polarization-type PID, Swanson et al. described that n-type IBC solar cells (Figure 1b) which have an n-type front surface undergo polarization-type PID under a positive bias with respect

to the grounded frame.<sup>[19,25]</sup> Also, there are reports on polarization-type PID under positive bias on the n-type rear surface of n-type PERT cells (Figure 1a)<sup>[22]</sup> and on the n-type emitter surface of Al-BSF cells (Figure 1d).<sup>[30,35]</sup> However, polarization-type PID occurs on p-type surfaces for negatively biased cells. This is, for example, on the p-type emitter surface of n-type PERT cells (Figure 1a)<sup>[20,23,24,26]</sup> and on the p-type rear surface of bifacial PERCs (Figure 1c).<sup>[29,33]</sup> This feature is unique to polarization-type PID. Other PID types, such as shunting-type PID, Na-penetration-type PID, and corrosion-type PID, are all related to  $Na^+$  ions and always occur in negatively biased cells relative to the grounded frame.<sup>[3–8,12]</sup> Therefore, this feature of polarization-type PID suggests that Na does not cause polarization-type PID directly.

Polarization-type PID is known to be the most rapidly occurring PID mode. We have reported from earlier work that polarization-type PID occurred within several seconds and that it almost saturated within a minute in a PID test where n-type PERT cells were biased with a  $-1000$  V at  $85^\circ\text{C}$ , as shown in Figure 2.<sup>[26]</sup> Here,  $J_{SC}/J_{SC,0}$ ,  $V_{OC}/V_{OC,0}$ ,  $FF/FF_0$ , and  $P_{max}/P_{max,0}$ , respectively, denote the initial-value-normalized  $J_{SC}$ ,  $V_{OC}$ , FF, and maximum output power. By stark contrast, shunting-type PID and corrosion-type PID, which are both caused by Na, require a much longer time: from several hours

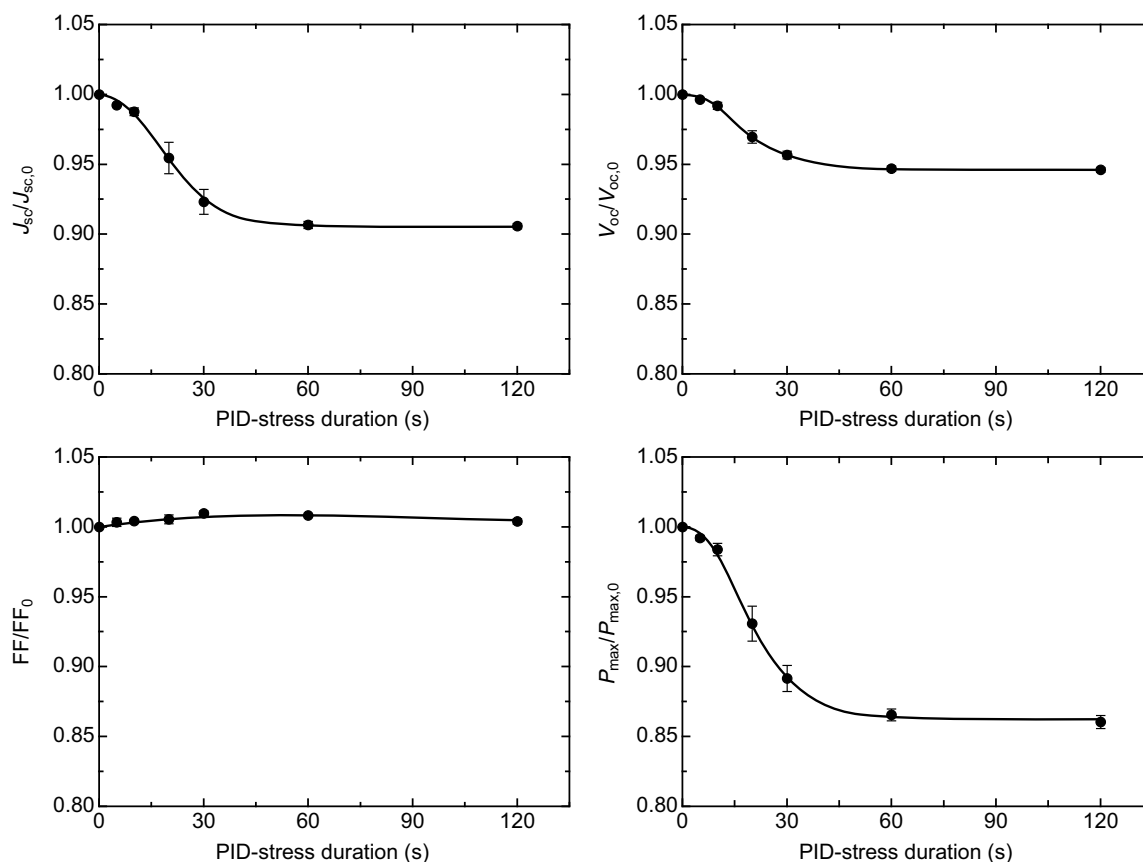


**Figure 2.** Dependences of  $J_{sc}/J_{sc,0}$ ,  $V_{oc}/V_{oc,0}$ ,  $FF/FF_0$ , and  $P_{max}/P_{max,0}$  of n-type PERT cell modules on the PID-stress duration. The PID test was conducted by application of a bias to cells from the cover glass surfaces. The bias and temperature in the PID tests were set respectively to  $-1000$  V and  $85^\circ\text{C}$ . Data points represent the mean values of three identical modules. Error bars correspond to the standard deviation of the mean. The solid lines are visual guides. Reproduced with permission.<sup>[26]</sup> Copyright 2018, The Japan Society of Applied Physics.

to several tens of days.<sup>[36]</sup> Therefore, rapid degradation caused by polarization-type PID, too, suggests that polarization-type PID is not related directly to Na. Note that n-type PERT cells reportedly also exhibit Na-related PID in long-term PID tests (see refs. [10,12,13] for details).

Additionally, polarization-type PID occurs more readily than the PID of other types. Hara et al.<sup>[20]</sup> reported that n-type PERT cells show polarization-type PID with a considerably low bias of  $-50$  V or at room temperature, as portrayed in **Figure 3**. This finding differs from those of other PID types that need high bias such as  $-600$  to  $-1000$  V and a high temperature such as  $60$ – $85$  °C, which then implies that polarization-type PID can occur even in small-scale systems such as rooftop PV systems. To date, PID is regarded as a phenomenon that occurs only in large-scale PV systems. However, regarding polarization-type PID, that consideration might not be correct. Polarization-type PID can occur in any PV system. Elucidations of the phenomenon and its countermeasures are very important. An earlier review<sup>[10]</sup> presents details of its countermeasures.

As one interesting feature, polarization-type PID is known not to occur in cells with single-layered  $\text{SiN}_x$  films.<sup>[30,31,35]</sup> Although n-type PERT cells with  $\text{SiN}_x/\text{SiO}_2$  stacked films show polarization-type PID,<sup>[20,23,26]</sup> n-type PERT cells without  $\text{SiO}_2$  exhibit no apparent polarization-type PID.<sup>[31]</sup> By contrast, standard Al-BSF cells (Figure 1d) are known to exhibit no polarization-type PID; however, Al-BSF cells with intentional  $\text{SiO}_2$  underneath  $\text{SiN}_x$  reportedly show polarization-type PID under a positive bias.<sup>[30,35]</sup> However, such  $\text{SiO}_2$  mitigates degradation for shunting-type PID.<sup>[37–39]</sup> This difference implies that the mechanisms of polarization-type PID and shunting-type PID are fundamentally different from one another.

As described above, polarization-type PID has unique features that are not observed for other PID types. The next section presents an explanation of a proposed model called the K-center model, which can explain the origin of the features, including how the model was conceived.

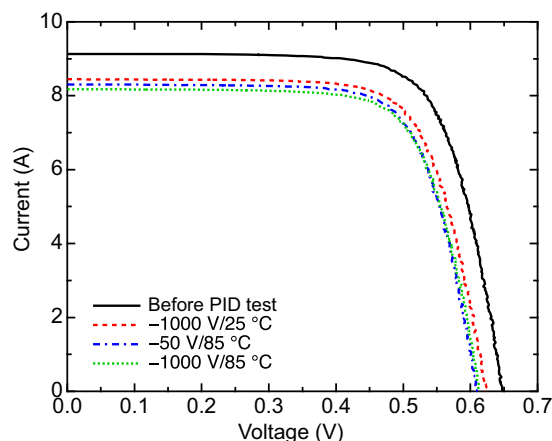


**Figure 3.** *I*–*V* curves of n-type PERT cell modules before and after the PID test for 2 h: before,  $-1000$  V at  $25$  °C,  $-50$  V at  $85$  °C, and  $-1000$  V at  $85$  °C. Reproduced with permission.<sup>[10]</sup> Copyright 2021, Wiley-VCH GmbH. Data were referred from earlier work.<sup>[20]</sup>

### 3. K-Center Model

Swanson et al. were the first to report polarization-type PID in n-type IBC cells.<sup>[19]</sup> That report indicated that polarization-type PID in n-type IBC cells occurs under positive bias. Swanson et al.<sup>[19]</sup> explained that the degradation results from electron accumulation in the front  $\text{SiN}_x$  layer. Accumulated electrons attract minority carriers, holes, toward the  $\text{SiN}_x/\text{n-type Si}$  interface and enhance surface recombination. Hara et al. proposed an almost identical model.<sup>[20]</sup> This model partly explains polarization-type PID behavior well. However, the model does not include the origin of accumulated charges.

The model we explain herein, called the K-center model,<sup>[23,26]</sup> a successor to those earlier models, involves the origin of accumulated charges. The K-center model comprehensively explains polarization-type PID and related phenomena. This section presents explanations of important details of the K-center model.

We first explain how we derived the K-center model from reported results and results obtained in our studies. In 2016, we started investigating polarization-type PID in n-type PERT cells with  $\text{SiN}_x/\text{SiO}_2$  stacked antireflection/passivation layers. First, we conducted usual PID tests of the cell modules. The bias was set to  $-1000$  V. The temperature was set to  $85$  °C. After the PID tests conducted during periods of 2 h to several hours, the cells showed polarization-type PID, as characterized by reductions in  $J_{\text{SC}}$  and  $V_{\text{OC}}$ . However, the degree of degradation was independent of the PID test duration. This finding suggests that the degradation was already saturated after the 2 h PID test. Then, we performed PID tests lasting from several seconds to several minutes. In the PID test, n-type PERT cells started to degrade within 5 s and saturated within 1–2 min.<sup>[23,26]</sup> This extremely high degradation rate clearly supports the opinion that polarization-type PID is not associated with  $\text{Na}^+$  drift. Instead, it is based on charge accumulation in front  $\text{SiN}_x$  because the drift time for  $\text{Na}^+$  across 80 nm  $\text{SiN}_x$  films is of approximately several tens of minutes.<sup>[36]</sup> Ion drift processes therefore cannot explain the highly rapid degradation rate.

The durations necessary for degradation to saturate and the leakage current density flowing between the cover glass and the cell separated by the encapsulant are also important hints for the origin of accumulated charges. As explained in the preceding paragraph, the degradation was saturated within 1–2 min. During the PID test, an almost constant leakage current was flowing with current density of  $\approx 0.1 \mu\text{A cm}^{-2}$ .<sup>[23,26]</sup> The integral of the leakage current density gives the areal density of positive charges supplied on the cell surface at a time. **Figure 4** shows that positive charges can be supplied on the cells' front surface with a density of up to  $\approx 10^{13} \text{ cm}^{-2}$  in 1–2 min. This finding suggests that the charge density causing polarization-type PID is limited to less than  $\approx 10^{13} \text{ cm}^{-2}$ . Additionally, our earlier simulation<sup>[23]</sup> reports that positive charges with a density of  $\approx 10^{12} \text{ cm}^{-2}$  reproduce polarization-type PID in n-type PERT cells. To explain these results, one must consider a mechanism by which the areal charge density in  $\text{SiN}_x$  is limited to approx.  $10^{12}$ – $10^{13} \text{ cm}^{-2}$ . Therefore, we considered K centers as candidates for chargeable centers.

The K centers are Si dangling bonds backbonded to three N atoms in  $\text{SiN}_x$ .<sup>[40–42]</sup> Also, K centers are present in typical  $\text{SiN}_x$  films in solar cells with density of  $\approx 10^{12}$ – $10^{13} \text{ cm}^{-2}$ .<sup>[43,44]</sup> One

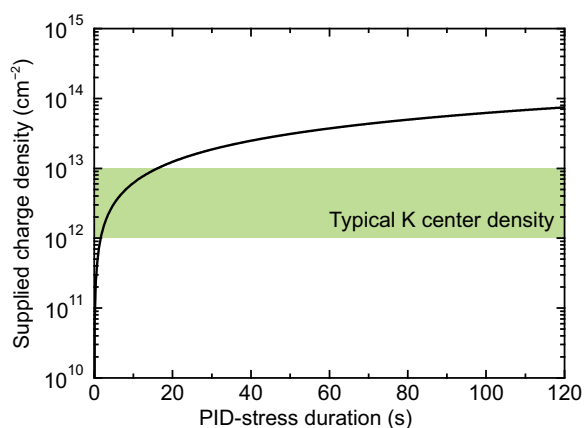


**Figure 4.** Dependence of the maximum density of supplied positive charges onto the cell surface on the PID-stress duration. Bias and temperature in the PID tests were set, respectively, to  $-1000$  V and  $85$  °C. It is noteworthy that not all charges contribute to the formation of  $K^+$  centers: most positive charges are regarded as neutralized on the finger electrode and busbar.

characteristic of K centers is that their charge state is manipulated by an externally applied voltage.<sup>[43,44]</sup> An electrically neutral K center ( $K^0$  center) has one electron. The K center is converted to a positively charged K center ( $K^+$  center) and a negatively charged K center ( $K^-$  center), respectively, by losing the electron that initially belongs to the  $K^0$  center and by receiving an electron (Figure 5a). Sharma et al.<sup>[44]</sup> reported that the K-center charge state can be manipulated by corona charging. The manipulated charge state is relatively stably maintained even after storage when  $SiO_2$  layers exist underneath the  $SiN_x$  films.<sup>[44]</sup> Work by Sharma's group provided important hints for building the K-center model. The work also provides important insight into the effects of  $SiO_2$  layers underneath  $SiN_x$ , as described in Section 4. We hypothesized that, in cases of polarization-type PID in n-type PERT cells, the electric-potential differences between aluminum frames and cells take electrons from  $K^0$  centers and  $K^-$  centers, leaving the  $K^+$  centers.<sup>[23,26]</sup> This model can consistently explain the experimentally observed rapid degradation and subsequent saturation and other related results reported to date. Details of this K-center model are explained hereinafter.

Figures 5b–d exhibit schematic diagrams of the K-center model for polarization-type PID in an n-type front-emitter PERT cell module. The figure portrays cross-sectional images obtained near the front surface of the n-type front-emitter PERT cell in the module undergoing polarization-type PID. The c-Si top surface is the p-type emitter with free electrons as minority carriers. Before applying a voltage,  $K^0$ ,  $K^+$ , and  $K^-$  centers are distributed in the front  $SiN_x$  passivation layer (Figure 5b). A schematic band diagram in the initial state is depicted in Figure 5e. During the negative bias application, a positively charged layer is created by polarization of the encapsulant and by transferred holes accumulated on the  $SiN_x$  surface (Figure 5c). This positively charged layer extracts electrons from  $K^0$  and  $K^-$  centers and leaves excess  $K^+$  centers in  $SiN_x$  (Figure 5d). The corresponding band diagram is illustrated schematically in Figure 5f. These excess  $K^+$  centers shift the

net charge of  $SiN_x$  toward positive. Thereby, minority carriers, electrons, are attracted to the  $SiN_x$ /c-Si interface. Interface recombination via interface defect states is enhanced, thereby causing reductions in  $J_{SC}$  and  $V_{OC}$ .

It is noteworthy that the model presented above is also applicable to  $SiN_x$ -passivated n-type surfaces, such as those n-type IBC solar cells, because K centers can also be charged negatively. For passivated n-type surfaces, the terms “negative”, “positive”, “positively charged”, “ $K^-$  centers”, “ $K^+$  centers”, “electrons”, and “holes” can be replaced, respectively, with “positive”, “negative”, “negatively charged”, “ $K^+$  centers”, “ $K^-$  centers”, “holes”, and “electrons” because PID occurs on p-type and n-type surfaces under opposite biases. Therefore, the model is not inconsistent with one feature: the bias direction causing polarization-type PID changes depending on the doping type of the cell surface.

This K-center model has explained experimentally obtained results related to polarization-type PID. The next section presents several such examples.

## 4. Explanations of Related Results by the K-Center Model

The K-center model can explain several results reported earlier. This fact supports the model validity. This section presents an attempt to explain the various reported results by the K-center model.

According to the model, the rapid degradation and subsequent saturation can be easily understood. We have reported that n-type PERT cell modules show rapid degradation and subsequent saturation within 1–2 min. The observed leakage current density (approx.  $0.1 \mu A cm^{-2}$ )<sup>[23,26]</sup> shows that a sufficient number of positive charges to cause a significant positive shift of net charge are supplied on the  $SiN_x$  surface. This finding is consistent with rapid degradation. Additionally, the density of supplied positive charges exceeds the typical K-center density in 1–2 min, which indicates that all  $K^0$  and  $K^-$  centers can be converted rapidly to  $K^+$  centers. The  $K^+$  center density reaches the upper limit, the density of the sum of  $K^0$ ,  $K^-$ , and  $K^+$  centers, in a very short time. This finding explains rapid saturation consistently. Additionally, using a cell-level PID test,<sup>[45,46]</sup> we confirmed similar saturation behavior of the positive fixed charges in  $SiN_x$  in a test structure.<sup>[26]</sup> Also, the saturated density of positive fixed charges was limited to  $\approx 10^{12} cm^{-2}$ ; it was in the same order as the K-center density.<sup>[26]</sup> These findings strongly support the model.

Some reports<sup>[23,26]</sup> have described that the saturation value of polarization-type PID is independent of the magnitude of the applied bias. In the PID test on n-type PERT cells at  $85$  °C, the degradation rate increased by changing the applied bias from  $-1000$  to  $-1500$  V. However, the degrees of degradation after degradation saturation were almost identical in both cases (Figure 6a).<sup>[23,26]</sup> This finding can be understood simply in terms of the K-center model. Based on the model, the density of the excess fixed charges realized by PID bias application is limited to the K-center density in  $SiN_x$  films. However, the degradation rate is sensitive to the magnitude of the applied bias because the



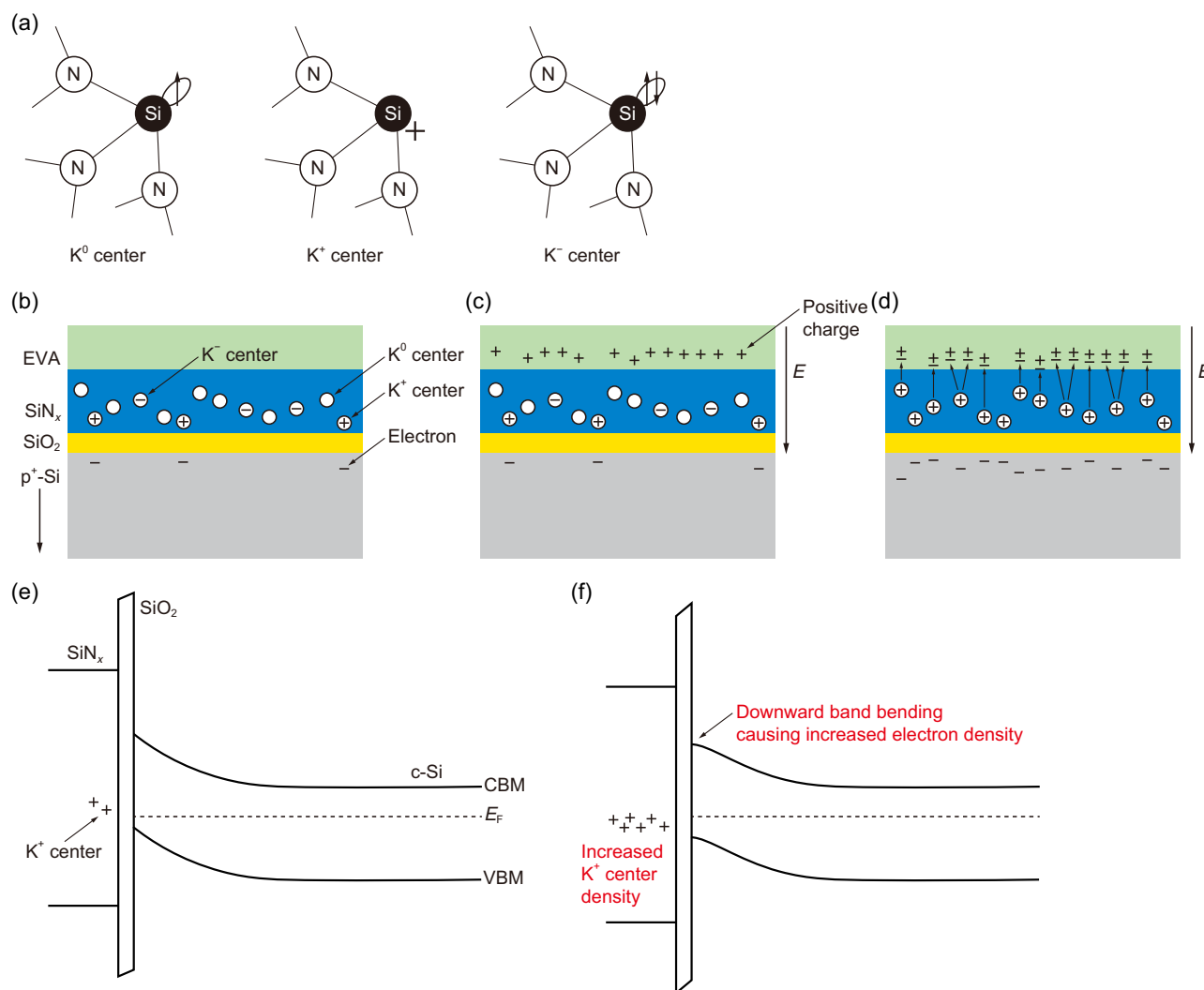


**Figure 5.** Schematic diagrams of K centers and the K-center model for polarization-type PID in n-type PERT cell modules. a) Schematic diagrams of a  $K^0$  center, a  $K^+$  center, and a  $K^-$  center. b–d) Cross-sectional images of a module near the EVA/cell interface. b) Before stressing, K centers exist in the front  $SiN_x$  film. c) During negative bias application, positive charges accumulate on the surface of the front  $SiN_x$  film. d) Positive charges subsequently extract electrons from  $K^0$  and  $K^-$  centers, leaving  $K^+$  centers. e, f) Schematic band diagrams of the n-type PERT cell e) before and f) after polarization-type PID.

charge injection rate, i.e., the leakage current density, depends on the magnitude of the applied bias.

A part of the PID types is recoverable by application of bias opposite to the bias causing degradation. Polarization-type PID, too, is known to be recovered similarly. If an upper limit exists for the excess charge density in  $SiN_x$ , then the time necessary for degraded solar cells to be recovered should be constant after degradation saturation. To verify this point, we conducted recovery tests by application of +1000 V at 85 °C to n-type PERT cells that were degraded in advance by –1000 V at 85 °C (Figure 6b).<sup>[26]</sup> Results have demonstrated that, despite the different PID-test times, the time necessary for complete recovery from degradation was the same. This observation is consistent with the hypothesis that an upper limit exists for the charge density in  $SiN_x$ . Consequently, this result supports the K-center model.

Effects of  $SiO_2$  layers underneath  $SiN_x$  on polarization-type PID have been investigated.<sup>[30–32,34,35]</sup> These reports indicate that  $SiO_2$  layers play important roles in generating polarization-type PID. We have proposed that  $SiO_2$  layers underneath  $SiN_x$  play a role in retaining excess accumulated charges at K centers. This hypothesis is derived from an earlier study that specifically examined a charge manipulation method with corona charging.<sup>[44]</sup> As described in that earlier report,<sup>[44]</sup> corona charging was found to shift the net charge of  $SiN_x$  films to both negative and positive. However, accumulated charges tended to dissipate via charge transport between the  $SiN_x$  films and the c-Si substrates when no  $SiO_2$  layer existed under the  $SiN_x$  films.<sup>[44]</sup> By contrast, the injected charges were maintained stably for a long time if  $SiO_2$  layers were present under the  $SiN_x$  films.<sup>[44]</sup> Since the publication of our earlier work,<sup>[23,26]</sup> many results that support our hypothesis have been reported.<sup>[30,31,34,35]</sup> Jonai et al. reported that

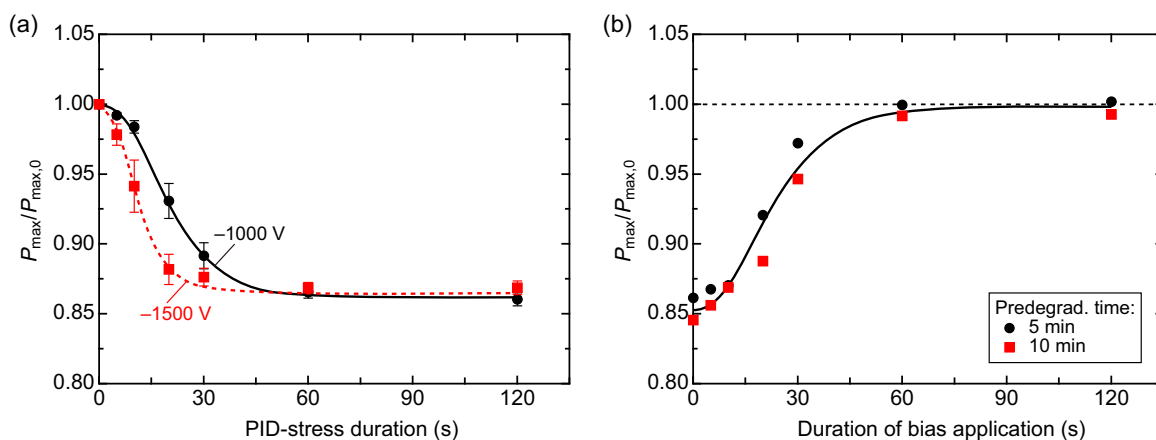


**Figure 6.** a) Applied-bias dependence of  $P_{\max}/P_{\max,0}$  of n-type PERT cell modules in PID tests at 85 °C. b) Regeneration n-type PERT cell modules degraded in earlier PID tests under a negative bias of –1000 V at 85 °C for 5 or 10 min. Regeneration tests were performed by application of a positive bias of +1000 V at 85 °C. Data points represent the mean values of three identical modules. The error bars correspond to the standard deviation of the mean. Solid and dashed lines are visual guides. Reproduced with permission.<sup>[26]</sup> Copyright 2018, The Japan Society of Applied Physics.

Al-BSF cells, which basically have no intentional  $\text{SiO}_2$  layers under  $\text{SiN}_x$ , show polarization-type PID when  $\text{SiO}_2$  is inserted between  $\text{SiN}_x$  and n-type emitters.<sup>[30,35]</sup> Suzuki et al.<sup>[31]</sup> demonstrated that n-type PERT cells without  $\text{SiO}_2$  layers exhibit no polarization-type PID. It is noteworthy that the n-type PERT cells without  $\text{SiO}_2$  layers show low initial performance. The method cannot be used as a preventive measure. A preventive measure based on a high refractive-index (RI) (Si-rich and highly conductive)  $\text{SiN}_x$  has been proposed.<sup>[47]</sup> The preventive measure mitigates polarization-type PID by promoting the dissipation of accumulated charges via charge transport between the Si-rich  $\text{SiN}_x$  and Si substrates. In addition, for this measure, we must use sufficiently thin  $\text{SiO}_2$  to permit electron tunneling through the  $\text{SiO}_2$ .<sup>[34]</sup> The RI does not affect the polarization-type PID behavior when the  $\text{SiO}_2$  ( $d_{\text{ox}}$ ) thickness is greater than 2 nm. However, for  $d_{\text{ox}}$  of approx. 1 nm, the degradation behavior depends greatly on the RI (Figure 7). Then, high RI mitigates

the polarization-type PID because thick  $\text{SiO}_2$  impedes charge transport between the  $\text{SiN}_x$  and Si substrates. This similarity between the roles of  $\text{SiO}_2$  in K-center-charge manipulation by corona charging and polarization-type PID indicates the model validity.

As described above, polarization-type PID occurs both on the p-type surface and the n-type surface because K centers can be charged both positively and negatively. The bias directions causing polarization-type PID are opposite for the p-type surface and the n-type surface. We have reported that the time necessary for polarization-type PID to saturate is longer on the n-type surface than on the p-type surface (Figure 8).<sup>[35]</sup> In fact, in Figure 8, the labeled “n-type” and “p-type” have, respectively, p-type and n-type front surfaces. Here, “n-type” and “p-type”, respectively, represent the behaviors of degradation on the p-type and n-type surfaces. This observation, too, can be explained consistently on the basis of the K-center model. For polarization-type PID on a p-type

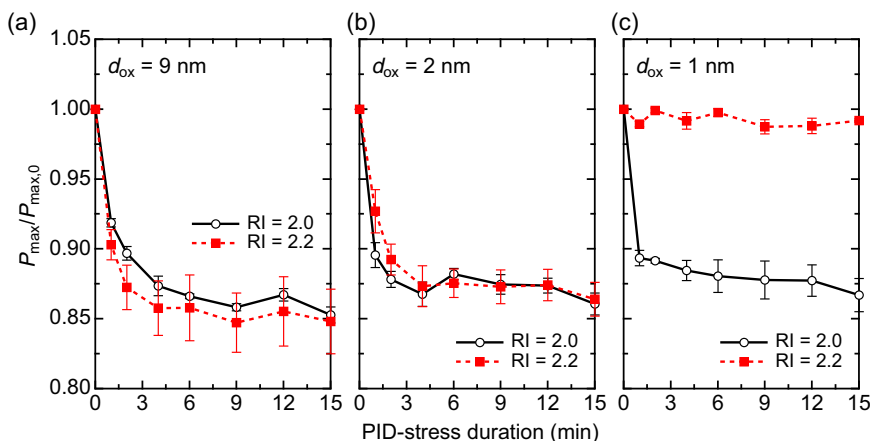


**Figure 7.** Influences of the RI of the front  $\text{SiN}_x$  layers on the  $P_{\max}/P_{\max,0}$  changes of n-type PERT cell modules undergoing PID tests: a)  $d_{\text{ox}} = 9$  nm; b)  $d_{\text{ox}} = 2$  nm; and c)  $d_{\text{ox}} = 1$  nm. Data points show mean values for the three modules. The error bar corresponds to the standard deviation of the mean. Solid and dashed lines are guides to the eye. Reproduced under the terms of the CC-BY 4.0 license.<sup>[34]</sup> Copyright 2022, The Authors. Published by Wiley-VCH GmbH.

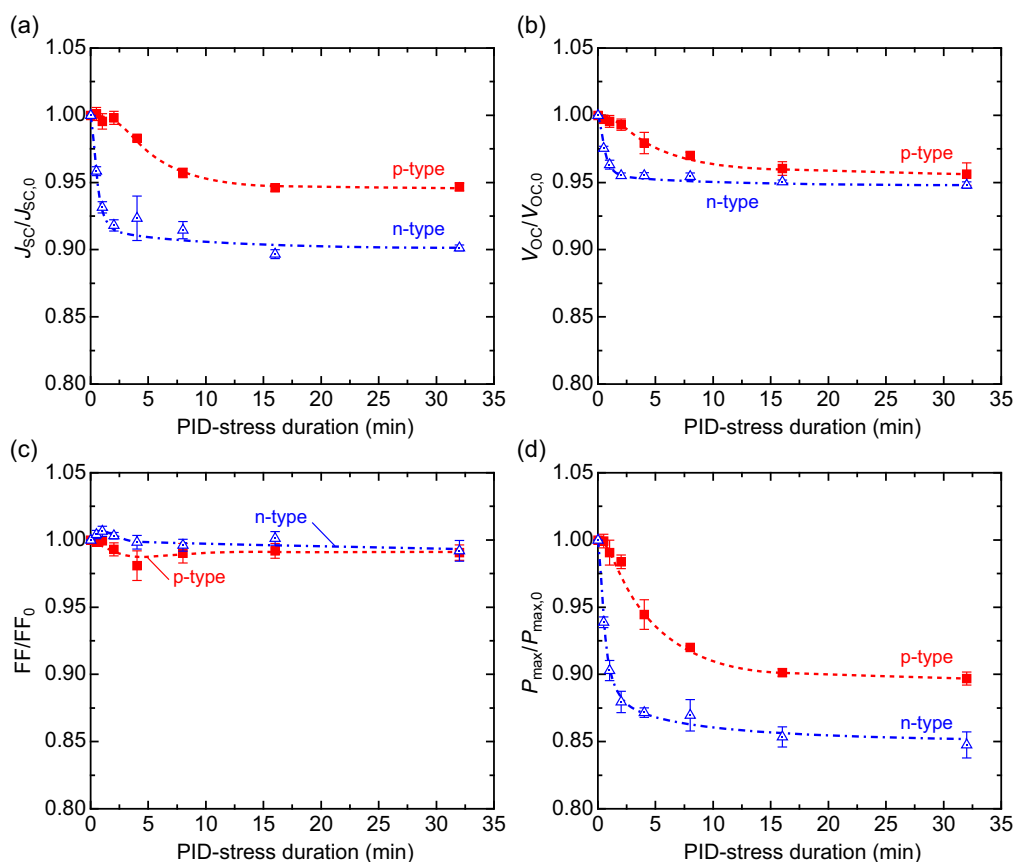


**Figure 8.** Dependence of a)  $J_{SC}/J_{SC,0}$ , b)  $V_{OC}/V_{OC,0}$ , c)  $FF/FF_0$ , and d)  $P_{max}/P_{max,0}$  of modules fabricated from p-type Al-BSF and n-type PERT cells with  $\text{SiN}_x/\text{SiO}_2$  double-layered passivation films on the PID-stress duration. The p-type cell modules were subjected to PID tests with a bias of +1000 V, whereas the n-type ones were subjected to PID tests with a bias of −1000 V. Both PID tests were performed in a chamber maintained at 85 °C. Data points show mean values for the three modules. The error bar corresponds to the standard deviation of the mean. Dashed and chain lines are guides to the eye. Reproduced under the terms of the CC-BY 4.0 license.<sup>[35]</sup> Copyright 2022, The Authors. Published by The American Chemical Society.

surface, degradation and its saturation are explained by positive charge accumulation at K centers and saturation of  $\text{K}^+$  centers, but they are limited by the density of K centers, including all the charge types. However, for polarization-type PID on the n-type surface, degradation and its saturation are explained by negative charge accumulation at K centers and saturation of  $\text{K}^-$  centers. The number of positive charges necessary to convert all the K centers into  $\text{K}^+$  centers is regarded as less than that of negative charges necessary to convert all the K centers into  $\text{K}^-$  centers because  $\text{SiN}_x$  on Si substrates is regarded as positively charged, initially.<sup>[48]</sup>

Other research groups have also attempted to explain their experimentally obtained results using the K-center model. Sporleder et al.<sup>[33]</sup> investigated polarization-type PID on the rear p-type surface of bifacial PERCs. Reportedly, as the PID-stress time increases, the  $J_{SC}$  and  $V_{OC}$  decrease once, then increase, and saturate. These degradation steps have been explained as depletion and inversion caused by an increase in the  $\text{K}^+$  center density and the saturation of the  $\text{K}^+$  center density. Habersberger and Hacke reported the effects of illumination on polarization-type PID in n-type PERT cells.<sup>[49]</sup> They have consistently

explained the recovery of degradation under illumination as a K-center neutralization process.

As described herein, the K-center model explains many reported results. Nevertheless, no result that is markedly inconsistent with the K-center model has been reported. This fact indicates the K-center model validity. We expect further validations and possible modifications of the model in the future. For example, the effects of the K-center density on the magnitude of polarization-type PID should be investigated. In addition, the respective effects of interlayers between  $\text{SiN}_x$  and c-Si substrates on polarization-type PID should be investigated further. As described herein, we mainly treat examples of n-type PERT cells with  $\text{SiO}_2$  interlayers. However,  $\text{AlO}_x$  too is frequently used as the interlayer for p-type surfaces. Additionally, more directly, we must perform in situ observation of the K-center charge state using operando electron spin resonance (ESR) spectroscopy.<sup>[50,51]</sup> ESR spectroscopy, which can detect  $\text{K}^0$  centers, was used for estimation of the K-center density in an earlier study.<sup>[26]</sup> By operando ESR spectroscopy, one can observe changes in the K-center charge state in  $\text{SiN}_x$  of cells undergoing polarization-type PID.



## 5. Conclusions

From this perspective, we have discussed the mechanistic aspects of polarization-type PID. First, we reviewed the characteristic features of polarization-type PID. Polarization-type PID has characteristic features that do not appear in the PID of other types. This finding suggests that the polarization-type PID mechanism differs markedly from that of shunting-type PID. Among them, the two following features were particularly important: the bias direction causing degradation is not always negative. It depends on the doping of the surface. Also, polarization-type PID is considerably faster than PID of other types. It saturates within a very short time. A model that is consistent with the characteristic features must be built.

Next, we explained the K-center model, including how the model was built. The degradation rate and the leakage current suggest that degradation results from accumulated charges with a density of approx.  $10^{12}$ – $10^{13}$  cm<sup>-2</sup> in SiN<sub>x</sub> layers. Additionally, the strong saturation behavior of polarization-type PID implies the existence of an upper limit for the density of accumulated charges. We made K centers as a candidate for the origins of accumulated charges that meet these criteria. K centers are present in SiN<sub>x</sub> for Si solar cells with areal density of  $\approx 10^{12}$ – $10^{13}$  cm<sup>-2</sup>. Additionally, K centers can be charged both positively and negatively by an applied electric field. Therefore, the K-center model has been built for explaining polarization-type PID, involving K-center charge injection and extraction processes.

In Section 4, we presented illustrative examples that are explained consistently within the K-center model. The K-center model explains the rapid degradation and subsequent saturation. Additionally, the model consistently explains other experimentally obtained results that have been reported to date. For example, the model consistently explains voltage independence of the magnitude of degradation after saturation, the recovery behavior, the effect of SiO<sub>2</sub> layers under SiN<sub>x</sub>, and the faster saturation of degradation on the p-type surface than on the n-type surface. Nevertheless, no results that are markedly inconsistent with the K-center model have been reported. This lack of inconsistent or contradictory results underscores the K-center model validity. As future studies, further validations and possible modifications of the model must be performed, elucidating, for example, K-center density effects on the magnitude of polarization-type PID and direct observation of the K-center charge state during polarization-type PID.

## Acknowledgements

This work was supported in part by the New Energy and Industrial Technology Development Organization, Japan, the Japan Society for the Promotion of Science KAKENHI (grant no. JP17J09648), and by the Japan Science and Technology Agency MIRAI (grants no. JPMJMI20C5, JPMJMI22C1).

## Conflict of Interest

The authors declare no conflict of interest.

## Keywords

photovoltaic modules, potential-induced degradations, reliability, silicon nitride, silicon solar cells

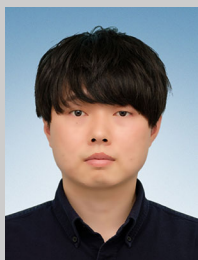
Received: October 31, 2022

Revised: November 30, 2022

Published online: December 29, 2022

- [1] K. Yamamoto, K. Yoshikawa, H. Uzu, D. Adachi, *Jpn. J. Appl. Phys.* **2018**, 57, 08RB20.
- [2] A. Richter, M. Hermle, S. W. Glunz, *IEEE J. Photovolt.* **2013**, 3, 1184.
- [3] S. Pingel, O. Frank, M. Winkler, S. Daryan, T. Geipel, H. Hoehne, J. Berghold, in *Proc. 35th IEEE Photovoltaic Specialists Conf.*, IEEE, Piscataway, NJ **2010**, pp. 2817–2822.
- [4] J. Berghold, O. Frank, H. Hoehne, S. Pingel, S. Richardson, M. Winkler, in *Proc. 25th European Photovoltaic Solar Energy Conf. Exhib./5th World Conf. Photovoltaic Energy Conversion*, WIP, Munich, Germany **2010**, pp. 3753–3759.
- [5] P. Hacke, M. Kempe, K. Terwilliger, S. Glick, N. Call, S. Johnston, S. Kurtz, I. Bennett, M. Kloos, in *Proc. 25th European Photovoltaic Solar Energy Conf. Exhib./5th World Conf. Photovoltaic Energy Conversion*, WIP, Munich, Germany **2010**, pp. 3760–3765.
- [6] V. Naumann, D. Lausch, A. Graff, M. Werner, S. Swatek, J. Bauer, A. Hähnel, O. Breitenstein, S. Großer, J. Bagdahn, C. Hagendorf, *Phys. Status Solidi: Rapid Res. Lett.* **2013**, 7, 315.
- [7] V. Naumann, D. Lausch, A. Hähnel, J. Bauer, O. Breitenstein, A. Graff, M. Werner, S. Swatek, S. Großer, J. Bagdahn, C. Hagendorf, *Sol. Energy Mater. Sol. Cells* **2014**, 120, 383.
- [8] S. Yamaguchi, A. Masuda, K. Ohdaira, *Jpn. J. Appl. Phys.* **2016**, 55, 04ES14.
- [9] W. Luo, Y. S. Khoo, P. Hacke, V. Naumann, D. Lausch, S. P. Harvey, J. P. Singh, J. Chai, Y. Wang, A. G. Aberle, S. Ramakrishna, *Energy Environ. Sci.* **2017**, 10, 43.
- [10] S. Yamaguchi, B. B. Van Aken, A. Masuda, K. Ohdaira, *Sol. RRL* **2021**, 5, 2100708.
- [11] E. Schneller, N. S. Shiradkar, N. G. Dhere, in *Proc. 40th IEEE Photovoltaic Specialists Conf.*, IEEE, Piscataway, NJ **2014**, pp. 3216–3219.
- [12] Y. Komatsu, S. Yamaguchi, A. Masuda, K. Ohdaira, *Microelectron. Reliab.* **2018**, 84, 127.
- [13] K. Ohdaira, Y. Komatsu, T. Suzuki, S. Yamaguchi, A. Masuda, *Appl. Phys. Express* **2019**, 12, 064004.
- [14] K. Sporleder, V. Naumann, J. Bauer, S. Richter, A. Hähnel, S. Großer, M. Turek, C. Hagendorf, *Phys. Status Solidi: Rapid Res. Lett.* **2019**, 13, 1900163.
- [15] K. Sporleder, V. Naumann, J. Bauer, S. Richter, A. Hähnel, S. Großer, M. Turek, C. Hagendorf, *Phys. Status Solidi A* **2019**, 216, 1900334.
- [16] K. Sporleder, V. Naumann, J. Bauer, S. Richter, A. Hähnel, S. Großer, M. Turek, C. Hagendorf, *Sol. Energy Mater. Sol. Cells* **2019**, 201, 110062.
- [17] S. Yamaguchi, C. Yamamoto, K. Ohdaira, A. Masuda, *Sol. Energy Mater. Sol. Cells* **2017**, 161, 439.
- [18] S. Yamaguchi, C. Yamamoto, K. Ohdaira, A. Masuda, *Prog. Photovolt. Res. Appl.* **2018**, 26, 697.
- [19] R. Swanson, M. Cudzinovic, D. DeCeuster, V. Desai, J. Jürgens, N. Kaminar, W. Mulligan, L. Rodrigues-Barbarosa, D. Rose, D. Smith, A. Terao, K. Wilson, in *Tech. Dig. 15th Photovoltaic Sci. Eng. Conf.*, **2005**, pp. 410–411.
- [20] K. Hara, S. Jonai, A. Masuda, *Sol. Energy Mater. Sol. Cells* **2015**, 140, 361.
- [21] A. Halm, A. Schneider, V. D. Mihailitchi, L. J. Koduvilukulathu, L. M. Popescu, G. Galbiati, H. Chu, R. Kopecek, *Energy Proc.* **2015**, 77, 356.

- [22] S. Yamaguchi, A. Masuda, K. Ohdaira, *Sol. Energy Mater. Sol. Cells* **2016**, 151, 113.
- [23] S. Yamaguchi, A. Masuda, K. Ohdaira, *Appl. Phys. Express* **2016**, 9, 112301.
- [24] S. Bae, W. Oh, K. D. Lee, S. Kim, H. Kim, N. Park, S.-I. Chan, S. Park, Y. Kang, H.-S. Lee, D. Kim, *Energy Sci. Eng.* **2017**, 5, 30.
- [25] T. Ishii, S. Choi, R. Sato, Y. Chiba, A. Masuda, *Prog. Photovolt. Res. Appl.* **2020**, 28, 1322.
- [26] S. Yamaguchi, K. Nakamura, A. Masuda, K. Ohdaira, *Jpn. J. Appl. Phys.* **2018**, 57, 122301.
- [27] W. Luo, Y. S. Khoo, J. P. Singh, J. K. C. Wong, Y. Wang, A. G. Aberle, S. Ramakrishna, *IEEE J. Photovolt.* **2018**, 8, 16.
- [28] W. Luo, P. Hacke, S. M. Hsian, Y. Wang, A. G. Aberle, S. Ramakrishna, Y. S. Khoo, *IEEE J. Photovolt.* **2018**, 8, 1168.
- [29] W. Luo, P. Hacke, K. Terwilliger, T. S. Liang, Y. Wang, S. Ramakrishna, A. G. Aberle, Y. S. Khoo, *Prog. Photovolt. Res. Appl.* **2018**, 26, 859.
- [30] S. Jonai, K. Nakamura, A. Masuda, *Appl. Phys. Express* **2019**, 12, 101003.
- [31] T. Suzuki, S. Yamaguchi, K. Nakamura, A. Masuda, K. Ohdaira, *Jpn. J. Appl. Phys.* **2020**, 59, SCCD02.
- [32] S. Yamaguchi, B. B. Van Aken, M. K. Stodolny, J. Löffler, A. Masuda, K. Ohdaira, *Sol. Energy Mater. Sol. Cells* **2021**, 226, 111074.
- [33] K. Sporleder, V. Naumann, J. Bauer, D. Hevisov, M. Turek, C. Hagendorf, *Sol. RRL* **2021**, 5, 2100140.
- [34] S. Yamaguchi, K. Nakamura, T. Semba, K. Ohdaira, K. Marumoto, Y. Ohshita, A. Masuda, *Energy Sci. Eng.* **2022**, 10, 2268.
- [35] S. Yamaguchi, S. Jonai, K. Nakamura, K. Marumoto, Y. Ohshita, A. Masuda, *ACS Omega* **2022**, 7, 36277.
- [36] M. Wilson, A. Savtchouk, P. Edelman, D. Marinskiy, J. Lagowski, *Sol. Energy Mater. Sol. Cells* **2015**, 142, 102.
- [37] H. Nagel, P. Saint-Cast, M. Glatthaar, S. W. Glunz, in *Proc. 29th European Photovoltaic Solar Energy Conf. Exhibition*, WIP, Munich, Germany **2014**, pp. 2351–2355.
- [38] Y. Yang, Y. F. Zhao, C. S. Tang, S. Zou, Y. Q. Yu, X. P. Ma, Y. Zhou, X. D. Su, Y. Xin, *Sol. Energy Mater. Sol. Cells* **2018**, 183, 101.
- [39] C.-H. Du, C.-H. Chen, C.-H. Lung, S.-Y. Chen, L.-Y. Li, Y.-H. Lin, J. A. Yeh, *ECS J. Solid State Sci. Technol.* **2015**, 4, P97.
- [40] W. L. Warren, J. Kanicki, F. C. Rong, E. H. Poindexter, *J. Electrochem. Soc.* **1992**, 139, 880.
- [41] P. M. Lenahan, S. E. Curry, *Appl. Phys. Lett.* **1990**, 56, 157.
- [42] W. L. Warren, P. M. Lenahan, *Phys. Rev. B* **1990**, 42, 1773.
- [43] K. J. Weber, H. Jin, *Appl. Phys. Lett.* **2009**, 94, 063509.
- [44] V. Sharma, C. Tracy, D. Schroder, S. Herasimenka, W. Dauksher, S. Bowden, *Appl. Phys. Lett.* **2014**, 104, 053503.
- [45] D. Lausch, V. Naumann, O. Breitenstein, J. Bauer, A. Graff, J. Bagdahn, C. Hagendorf, *IEEE J. Photovolt.* **2014**, 4, 834.
- [46] S. Yamaguchi, K. Ohdaira, *Sol. Energy* **2017**, 155, 739.
- [47] G. J. M. Janssen, M. K. Stodolny, B. B. Van Aken, J. Löffler, M. W. P. E. Lamers, K. J. J. Tool, I. G. Romijn, *IEEE J. Photovolt.* **2019**, 9, 608.
- [48] R. Hezel, K. Jaeger, *J. Electrochem. Soc.* **1989**, 136, 518.
- [49] B. M. Habersberger, P. Hacke, *Prog. Photovolt. Res. Appl.* **2022**, 30, 455.
- [50] T. Watanabe, T. Yamanari, K. Marumoto, *Commun. Mater.* **2020**, 1, 96.
- [51] D. Xue, M. Saito, I. Osaka, K. Marumoto, *npj Flex. Electron.* **2022**, 6, 22.



**Seira Yamaguchi** received his Ph.D. in materials science from the Japan Advanced Institute of Science and Technology, Japan, in 2019. He joined Toyota Technological Institute as a postdoctoral researcher, in 2019, and joined Niigata University as an assistant professor, in 2020. His research work mainly covered the investigation of potential-induced degradation in n-type crystalline-silicon solar cells and the fabrication of high-quality passivating contact materials. He has been an assistant professor at the University of Tsukuba since 2021. His current research interests include the characterization of carbon fiber-reinforced plastics, perovskite solar cells, and organic semiconductor devices by operando electron spin resonance spectroscopy.



**Atsushi Masuda** received his Ph.D. degree in engineering from Kanazawa University, Japan, in 1996. In 1996, he joined the Japan Advanced Institute of Science and Technology; in 2005, he joined the National Institute of Advanced Industrial Science and Technology; and in 2020, he joined Niigata University. He is currently a professor, Graduate School of Science and Technology, and a deputy director, Interdisciplinary Research Center for Carbon-Neutral Technology, Niigata University. His main research fields are photovoltaics and thin-film electronic materials. He is a vice president of the Japan Photovoltaic Society and a senior member of the Japan Society of Applied Physics.



**Kazuhiro Marumoto** received his Ph.D. degree in science from Osaka University, Japan, in 1997. He worked as an assistant professor at Nagoya University, Japan, and an associate professor at the University of Tsukuba, Japan. He is a professor of Division of Materials Science and Tsukuba Research Center for Energy Materials Science at the University of Tsukuba, Japan. He has published more than 180 papers in journals, and served as a director, the Society of Electron Spin Science and Technology, Japan. His research topics are the characterization and development of organic and hybrid semiconductor devices by operando electron spin resonance.



**Keisuke Ohdaira** received his Ph.D. from the University of Tokyo, in 2004. He then moved to Tohoku University and worked as a postdoctoral researcher (2004–2005). He became an assistant professor (2005–2011) in Japan Advanced Institute of Science and Technology (JAIST), and promoted to an associate professor (2012–2018) and to a professor (2018–) in JAIST. He received the best paper award of the 27th International Photovoltaic Science and Engineering Conference (PVSEC-27), in 2017. His research topics are related to catalytic chemical vapor deposition, flash lamp annealing for poly-Si formation, and potential-induced degradation of photovoltaic modules.